Earth and Planetary Science Letters, 47 (1980) 11–20

[6]

THE EFFECT OF MANGANESE ON OLIVINE-QUARTZ-ORTHOPYROXENE STABILITY

STEVEN R. BOHLEN[1] *, ARTHUR L. BOETTCHER[2], WAYNE A. DOLLASE[3] and ERIC J. ESSENE[1]

[1] *Department of Geology and Mineralogy, University of Michigan, Ann Arbor, MI 48104 (U.S.A.)*
[2] *Institute of Geophysics and Planetary Physics and Department of Earth and Space Sciences, University of California at Los Angeles, Los Angeles, CA 90024 (U.S.A.)*
[3] *Department of Earth and Space Sciences, University of California at Los Angeles, Los Angeles, CA 90024 (U.S.A.)*

Received March 19, 1979
Revised version received October 23, 1979

The effect of manganese on the stability of ferrosilite relative to fayalite + quartz has been experimentally determined to assess its importance to orthopyroxene barometry. Reaction reversals in a piston-cylinder apparatus were obtained to within 0.1-kbar intervals indicating instability of $Fs_{95}Rh_5$ below 10.3, 10.9, 11.4, 12.2, 12.9, 13.7 kbar and $Fs_{90}Rh_{10}$ below 9.8, 10.4, 10.9, 11.6, 12.4 and 13.2 kbar at 750, 800, 850, 900, 950 and 1000°C, respectively. Each mole % $MnSiO_3$ extends the pyroxene stability by approximately 0.12 kbar relative to $FeSiO_3$. Electron microprobe analyses of run products indicate a small preference of Mn for pyroxene over olivine with $K_D^{opx\text{-}oliv}{}_{Mn\text{-}Fe}$ = 1.2–1.5, similar to values observed for natural pairs. Mössbauer spectra are consistent with a random distribution of Mn between the M1 and M2 sites in the orthopyroxene. These experimental data allow downward revision of pressure estimates based on the orthopyroxene barometer in areas where Mn is a significant component in orthopyroxene.

1. Introduction

Reactions involving minerals with solid solutions have long been recognized for their potential in determining or limiting pressure and temperature. Minor components can shift the stabilities of reactants and products of a solid-solid reaction over a wide range of pressures and temperatures. Theoretically, these types of reactions should be much more useful than univariant or nearly univariant that result from limited solid solution. Unfortunately, there are rarely sufficient activity data available to allow calculation of the effect of additional components on a given reaction boundary, and the usefulness of many potential barometers and thermometers is greatly reduced unless experimental data can be obtained. It has been shown in the previous paper [1] that the reaction olivine + quartz ⇆ orthopyroxene is of potential use as a geobarometer, but activity data are unavailable or insufficiently well refined to unambiguously calculate the effects of solid solutions. Order-of-magnitude calculations suggest that additional components can extend the stability of pyroxene to lower pressures. Smith [2,3] experimentally investigated the effect of MgO in olivine and in orthopyroxene in the system Mg_2SiO_4-Fe_2SiO_4-SiO_2. He showed that 30 mole % $MgSiO_3$ stabilizes the pyroxene over olivine + quartz at 900°C and atmospheric pressure; in the Mg-free system (at 900°C), ferrosilite is stable only above 12.6 kbar [1]. Other components including Mn, Ca, Na, Al, Ti, and Fe^{3+} will also probably enhance pyroxene stability, because they are preferentially concentrated in the pyroxene. $MnSiO_3$ is a major

* Present address: Institute of Geophysics and Planetary Physics, University of California, Los Angeles, Los Angeles, CA 90024, U.S.A.

Institute of Geophysics and Planetary Physics Publication No. 1885. Mineralogy Laboratory, University of Michigan, Contribution No. 348.

impurity in some natural Fe-rich orthopyroxenes, such as at Lofoten, Norway [4], where it is the most significant additional component. Consequently, the writers have undertaken piston-cylinder experiments to calibrate the effects of 5 and 10 mole % rhodonite solid solution on the stability of Fe-rich orthopyroxene.

2. Experimental methods

With a few exceptions the experimental methods used in this study are identical to those described in detail in the previous paper. Starting materials were prepared from electrolytically reduced iron powder, synthetic Mn_3O_4 and Brazilian quartz. Equimolar mixtures of fayalite$_{95}$ tephroite$_5$ + quartz and fayalite$_{90}$ tephroite$_{10}$ + quartz were synthesized in a CO_2/H_2 gas-mixing furnace and served as one set of starting materials. $Fa_{95}Te_5$ + quartz and $Fa_{90}Te_{10}$ + quartz were reacted in a piston-cylinder device (20 kbar, 900°C, 1–2 wt.% H_2O) to synthesize ferrosilite$_{95}$ rhodonite$_5$ and ferrosilite$_{90}$ rhodonite$_{10}$, respectively. These served as the other set of starting materials. Starting materials were analyzed by optical, X-ray, electron microprobe and Mössbauer techniques to insure that they were stoichiometric and homogeneous. The experimental apparatus, furnace assemblies, capsules, run procedures and criteria for reaction direction for the piston-cylinder experiments are also identical to those discussed in the previous paper. For most runs (see Table 1 and 2 for run data) equimolar mixtures of $Fs_{95}Rh_5$–$Fa_{95}Te_5$ + quartz and $Fs_{90}Rh_{10}$–$Fa_{90}Te_{10}$ + quartz were used for determination of the 5 and 10 mole % boundaries respectively. To reverse the K_D, an initially high-K_D starting

TABLE 1

Run data (5 mole % Mn_2SiO_4, $MnSiO_3$)

Run No.	T (°C)	P (kbar)	Duration (hours)	Products
62	750	10.5	26.3	*opx* + oliv + qtz
64	750	10.3	24	*opx* + oliv + qtz
67	750	10.2	23.5	*oliv* + *qtz* + opx
55	800	11.0	23.5	*opx* + (oliv + qtz)
58	800	10.8	24	*oliv* + *qtz* + (opx)
61	800	10.9	24	*oliv* + *qtz* + opx
63	850	11.5	24	*opx* + (oliv + qtz)
70	850	11.4	24	*oliv* + *qtz* + (opx)
54	900	12.0	24	*oliv* + *qtz* + (opx)
57	900	12.2	24	*oliv* + *qtz* + opx
1133 *	900	12.2	10	*oliv* + *qtz* + opx
60	900	12.3	24	*opx* + (oliv + qtz)
65	950	13.1	19	*opx* + (oliv + qtz)
68	950	12.9	19.5	*opx* + oliv + qtz
69	950	12.8	22.5	*oliv* + *qtz* + opx
37	1000	12.5	27	*oliv* + *qtz*
40	1000	12.9	22	*oliv* + *qtz*
48	1000	13.2	24	*oliv* + *qtz* + (opx)
50	1000	13.5	23	*oliv* + *qtz* + (opx)
51	1000	13.4	21.5	*oliv* + *qtz* + (opx)
52	1000	13.6	24	*oliv* + *qtz* + opx
56	1000	13.7	22.5	*oliv* + *qtz* + opx
59	1000	13.8	25	*opx* + (oliv + qtz)

Italics show the dominant phase(s).

Parentheses indicate very minor to trace amounts.

* Starting material was equal-weight mixture of $Fe_{1.80}Mn_{0.20}Si_2O_6$ and Fa_{100} (+ SiO_2).

TABLE 2

Run data (10 mole % Mn_2SiO_4, $MnSiO_3$)

Run No.	T (°C)	P (kbar)	Duration (hours)	Products
77	750	9.5	23.5	*oliv + qtz* + (opx)
80	750	9.9	24	*opx* + oliv + qtz
84	750	9.8	24	*oliv + qtz* + opx
1152	750	23.0	193	*opx* + qtz
72	800	10.3	24	*oliv + qtz* + (opx)
79	800	10.5	23.5	*opx* + oliv + qtz
83	800	10.4	23.5	*oliv + qtz* + (opx)
95	850	11.0	24	*opx* + (oliv + qtz)
96	850	10.8	21.5	*oliv + qtz* + (opx)
73	900	11.7	21	*opx* + (oliv + qtz)
78	900	11.5	29	*oliv + qtz* + (opx)
87	900	11.6	22	*opx* + oliv + qtz
76	950	12.4	22.5	*opx* + (oliv + qtz)
82	950	12.2	22	*oliv + qtz* + (opx)
86	950	12.3	24	*oliv + qtz* + opx
75	1000	13.3	23	*opx* + (oliv + qtz)
81	1000	13.0	19	*oliv + qtz* + (opx)
85	1000	13.2	23	*opx* + oliv + qtz

Italics show dominant phase(s).
Parentheses indicate very minor to trace amounts.

material ($Fs_{90}Rh_{10}$–Fa_{100} + quartz) of average composition $Fs_{95}Rh_5$ was used. Microprobe analyses of run products were obtained using equipment and techniques described in the previous paper. The analyses are listed in Tables 3 and 4. Each analysis represents an average of 4–5 points taken on different grains in each run product. Maximum deviations among the points within a single analysis were less than 1.5–2% of the amount present for each element analyzed.

Mössbauer spectra of a few powdered run products were obtained at room temperature using a constant acceleration, mechanically driven Mössbauer spectrometer. Samples of 50–100 mg were used with a 10 mCi ^{57}Co in Pd source. Duplicate spectra were recorded in 512 channels of a multichannel analyzer using a velocity increment of 0.03 mm per second per channel. Counting times were sufficient to obtain several million counts per channel and peak dips on the order of 10^5 counts. The spectra were fit with lorentzian doublets constrained to equal widths for the low- and high-velocity components. Chi-squared and additional goodness-of-fit parameters suggested by Ruby [15] were calculated for each fitted spectrum.

3. Experimental results and discussion

The effect of 5 and 10 mole % rhodonite solid solution on the stability of ferrosilite has been calibrated at 50°C intervals from 750 to 1000°C, and the results are shown in Figs. 1 and 2. For comparison, the end-member reaction boundary is also shown. It can be seen that 5 and 10 mole % rhodonite extend the stability of the pyroxene by nearly 0.6 and 1.2 kbar, respectively, relative to fayalitic olivine + quartz. All three reaction boundaries change slope from approximately dP/dT = 10 bar/°C to dP/dT = 15 bar/°C, where they intersect the α-β quartz transition. Our indirect location of the α-β quartz transition agrees well with the determination of Cohen and Klement [5]. We have obtained microprobe analyses of run products of coexisting orthopyroxene and olivine to determine the partitioning of manganese. The analyses are compiled in Tables 3 and 4, and the

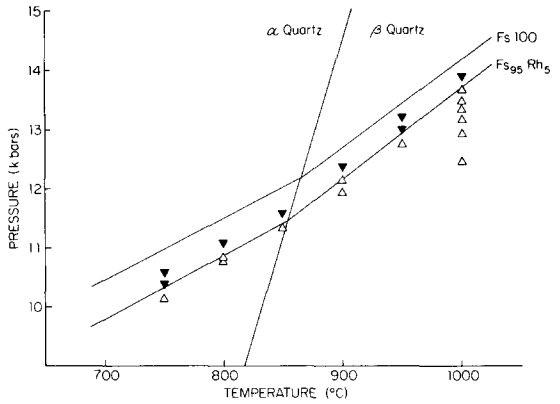

Fig. 1. *P-T* projection showing the effect of 5 mole % rhodonite solid solution on Fe-rich pyroxene stability. ▼ indicates that pyroxene grew from olivine + quartz. △ indicates that olivine + quartz formed from pyroxene breakdown. The ferrosilite stability [1] is shown for reference.

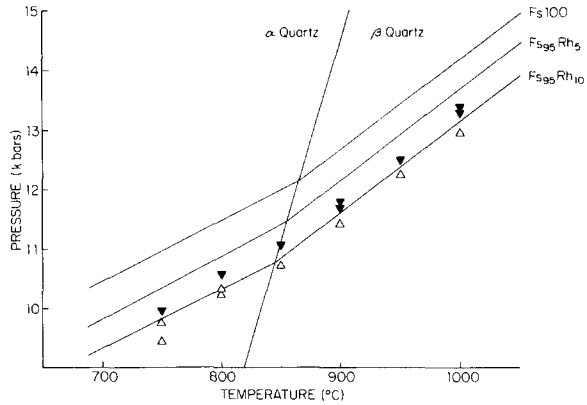

Fig. 2. *P-T* projection showing the effect of 10 mole % rhodonite solid solution on Fe-rich pyroxene stability. Symbols indicate reaction direction as in Fig. 1. For reference the stability curves for ferrosilite and ferrosilite –5 mole % rhodonite are shown.

compositions of coexisting phases are represented graphically in Fig. 3. At 900°C we have reversed the K_D * (runs 57 and 1133, Table 1) by using initially low-K_D and high-K_D starting materials in runs at the same *P-T*. The K_D at 900°C is constrained between $K_D^{\text{opx-oliv}}{}_{\text{Mn-Fe}} = 1.2–1.5$, consistent with most natural Fe-rich orthopyroxene-olivine pairs [6–8]. At other temperatures half-reversals of K_D indicate that the $K_D^{\text{opx-oliv}}{}_{\text{Mn-Fe}}$ is greater than 1.15 in all but one of the temperatures investigated. We have also obtained Mössbauer spectra to determine any cation ordering in our experimental products. This amounts to determining the intracrystalline K_D which, together with the intercrystalline K_D, are important parameters when attempting to thermodynamically model this system.

Mössbauer spectra were obtained on five orthopyroxene samples synthesized in 24-hour runs at 20–23 kbar, and having $MnSiO_3$ components of 0% (900°C), 5% (750 and 900°C) and 10% (750 and 900°C). The limit of detectability of Fe^{3+} in these samples under the measurement conditions employed is estimated as less than 1% of the iron present and no Fe^{3+} was detected in any sample. The 10 mole % samples showed 1–2% of the iron to be present in an impurity phase, apparently garnet. Other than this minor component, the samples were single-phase orthopyroxene.

The Mössbauer spectrum of orthopyroxene, near the ferrosilite end-member composition, consists of two slightly and asymmetrically separated ferrous doublets. The outer doublet results from Fe^{2+} in the octahedrally coordinated M1 site of the orthopyroxene structure and the inner doublet results from Fe^{2+} in the more distorted M2 structural site. The evidence for this assignment and a summary of previous orthopyroxene Mössbauer spectra is given by Bancroft [14]. For the samples measured here, the average isomer shifts and quadrupole splittings (Fe in M1 IS_{Pd} = 0.97 mm/s, Qs = 2.50 mm/s; Fe in M2 IS_{Pd} = 0.92 mm/s, Qs = 1.92 mm/s) are closely similar to previously reported values. Observed peak widths varied slightly from 0.29 mm/s for both the inner and outer doublet at pure $FeSiO_3$ to 0.30 for the inner and 0.33 for the outer doublet at 10 mole % Mn component.

Site occupancies of Fe^{2+} were calculated from the fitted spectral peak areas assuming equal recoil-free fractions for the two sites. The occupancy estimates and their least-squares fitting errors for each com-

* K_D, the distribution coefficient is defined as the ratio of cations in coexisting minerals. $K_D^{\text{opx-oliv}}{}_{\text{Mn-Fe}}$ reflects the relative proportions of Mn and Fe in orthopyroxene and olivine and is calculated: $K_D^{\text{opx-oliv}}{}_{\text{Mn-Fe}} = [Mn^{opx}/Fe^{opx}]\,[Fe^{oliv}/Mn^{oliv}]$.

TABLE 3

Microprobe analyses of run products for 5 mole % Rh_{ss} and Te_{ss} starting composition

Run No.	62 Opx	62 Oliv	64 Opx	64 Oliv	55 Opx	55 Oliv	58 Opx	
Temperature (°C)	750	750	750	750	800	800	800	
SiO_2	46.9	30.6	46.5	30.5	46.8	30.3	45.9	
MnO	2.8	3.2	2.8	3.3	2.7	3.2	2.7	
FeO	51.1	66.0	50.9	65.8	51.1	66.4	50.7	
Total	100.8	99.8	100.2	99.6	100.6	99.9	99.3	
Si	2.04	1.04	2.04	1.0	2.04	1.03	2.03	
Mn	0.10	0.09	0.10	0.09	0.10	0.09	0.10	
Fe	1.86	1.87	1.86	1.87	1.86	1.88	1.87	
Run No.	58 Oliv	63 Opx	70 Oliv	57 Opx	57 Oliv	60 Opx	1133 Opx	
Temperature (°C)	800	850	850	900	900	900	900	
SiO_2	30.4	46.6	30.4	46.4	31.3	46.6	45.6	
MnO	3.2	2.7	3.5	2.8	3.0	2.7	3.1	
FeO	66.2	51.1	66.1	51.1	66.4	51.1	51.3	
Total	99.8	100.4	100.0	100.3	99.7	100.4	100.0	
Si	1.03	2.04	1.03	2.02	1.03	2.03	2.00	
Mn	0.09	0.10	0.10	0.11	0.09	0.10	0.12	
Fe	1.88	1.87	1.87	1.87	1.88	1.87	1.88	
Run No.	1133 Oliv	68 Opx	68 Opx	69 Opx	69 Oliv	56 Oliv	59 Opx	59 Oliv
Temperature (°C)	900	950	950	950	950	1000	1000	1000
SiO_2	29.8	46.3	30.7	46.1	30.6	30.1	45.5	30.3
MnO	2.7	2.8	3.1	2.9	3.1	3.5	2.9	3.1
FeO	67.5	51.2	66.9	51.3	66.3	67.1	51.9	67.0
Total	100.0	100.3	100.7	100.3	100.0	100.8	100.3	100.4
Si	1.01	2.02	1.03	2.02	1.03	1.02	1.99	1.02
Mn	0.08	0.11	0.09	0.11	0.09	0.10	0.11	0.09
Fe	1.91	1.87	1.88	1.87	1.88	1.88	1.90	1.89

position are given in Table 5. The equal occupancy, within experimental error, of the two sites for the pure iron end-member lends confidence in the assumption of equal recoil-free fractions. The spectra are of sufficient quality that the probable errors in site occupancy, even considering small additional systematic errors, are only a few percent of the amount of iron present. Mn occupancies and any resulting Mn site preference, however, rests on the difference between the iron contents of the two sites. As these differences are small in all cases and only slightly larger than the estimated fitting imprecision, a Mn site preference, if any, is not well determined by these data. As shown in Table 5, all the spectra are consistent with a random distribution of Mn between the M1 and M2 orthopyroxene sites. The deviations of the fitted results from those expected in the case of complete ordering of Mn in either the M2 or the M1 site are generally greater and probably beyond reasonable experimental error.

In addition to site occupancies, the activity of fayalite component in tephroite solid solution and

TABLE 4

Microprobe analyses of run products for 10 mole % Rh_{ss} and Te_{ss} starting composition

Run No.	80 Opx	80 Oliv	79 Opx	79 Oliv	73 Opx	78 Oliv	87 Oliv
Temperature (°C)	750	750	800	800	900	900	900
SiO_2	44.9	29.3	45.1	29.9	44.6	29.0	45.6
MnO	5.4	6.5	5.4	6.6	5.3	6.5	5.5
FeO	49.5	65.2	48.8	65.1	49.8	63.4	49.3
Total	99.8	101.0	99.3	101.6	99.7	98.9	100.4
Si	1.98	0.99	2.00	1.00	1.97	0.99	2.00
Mn	0.20	0.19	0.21	0.19	0.20	0.19	0.21
Fe	1.82	1.83	1.79	1.81	1.83	1.82	1.80
Run No.	87 Oliv	76 Opx	82 Oliv	86 Opx	86 Oliv	75 Opx	81 Oliv
Temperature (°C)	900	950	950	950	950	1000	1000
SiO_2	28.7	44.7	30.4	44.7	29.3	44.9	29.3
MnO	6.2	5.4	7.1	5.4	6.2	5.3	6.9
FeO	64.4	49.7	63.0	48.3	64.8	49.8	64.0
Total	99.3	99.8	100.5	98.4	100.3	100.0	100.2
Si	0.98	1.97	1.02	1.99	0.99	1.97	1.00
Mn	0.18	0.20	0.20	0.21	0.18	0.20	0.20
Fe	1.84	1.83	1.78	1.80	1.83	1.83	1.80

the distribution coefficient (K_D) for Fe-Mn between olivine and orthopyroxene must also be known to properly evaluate the mixing properties of $MnSiO_3$ in $FeSiO_3$ from the experimental data presented. These variables are either unknown or are only poorly defined, although the site-occupancy data are of some limited value. The Mössbauer spectra of the run products are consistent with a random distribution of Mn in the M2 and M1 sites of orthopyroxene. Yet in natural materials, Mn shows a strong preference for the M2 site in orthopyroxene. Because the inferred mixing parameters will be dependent on site occupancies, the differences between experimental and natural materials must be considered. Because of uncertainties in K_D, the activity of fayalite component in Fe-Mn olivines, and site occupancies, the existing data are insufficient to unambiguously define the mixing parameters of Fe-Mn orthopyroxene solutions. However, the data do allow calculation of models that make specific predictions about K_D and Fe-Mn mixing parameters in orthopyroxene, which can be tested in future experiments. Table 6 shows models calculated to demonstrate certain features of Fe-Mn orthopyroxene mixing. * Models 1a and 1b show calculated activity coefficients for $FeSiO_3$ component in orthopyroxene ($\gamma^{opx}_{FeSiO_3}$) assuming that the K_D

* The models have been calculated assuming an ordered and disordered pyroxene where activity of ferrosilite in the orthopyroxene ($a^{opx}_{FeSiO_3}$) is given by $(\gamma^{opx}_{FeSiO_3} X^{opx}_{Fe})^2$ for the disordered case and by $\gamma^{opx}_{FeSiO_3}(1 - X^{M2}_{Mn})$ for the ordered case. The activity of fayalite in olivine (a^{oliv}_{Fa}) is calculated as $(\gamma^{oliv}_{Fe_2SiO_4} X^{oliv}_{Fe})^2$ in all cases. ΔP is then calculated:

$$\Delta P \simeq \frac{-RT(41.84)}{\Delta V_{P,T}} \ln(a^{oliv}_{Fa}/a^{opx}_{Fs})$$

for the reactions:

$Fe_{2-x}Mn_xSiO_4 + SiO_2 = 2\ Fe_{1-y}Mn_ySiO_3$

(disordered pyroxene)

$Fe_{2-x}Mn_xSiO_4 + SiO_2 = Fe_{2-y}Mn_ySi_2O_6$

(ordered pyroxene)

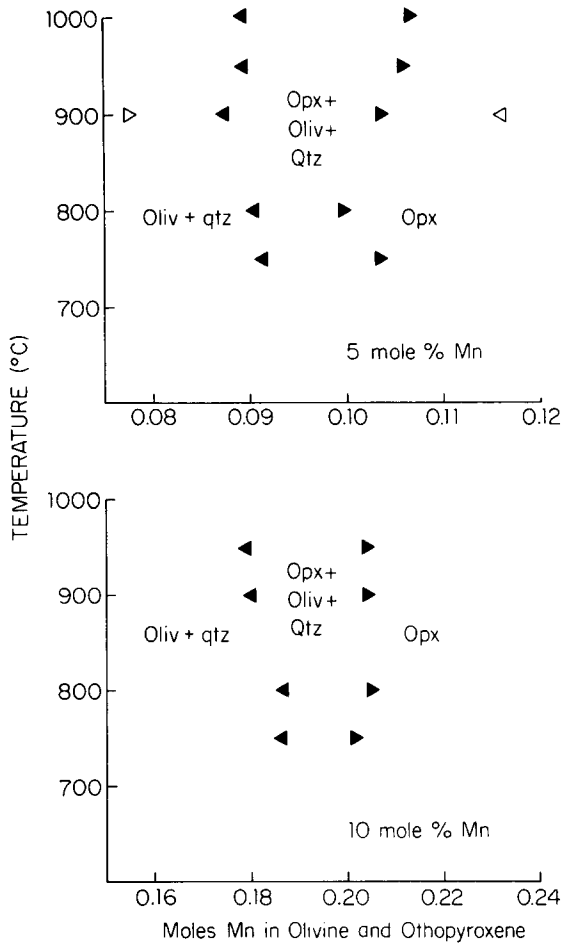

Fig. 3. T-X projection of compositions of coexisting Fe-Mn olivines and pyroxenes in run products as determined by electron microprobe analyses (see Table 3 and 4). ◂ ▸ indicate the final compositions of olivine and orthopyroxene with starting composition of $Fa_{95}Te_5$ and $Fs_{95}Rh_5$. ▷ ◁ indicate the final compositions of olivine and orthopyroxene with starting composition of $Fa_{100}Te_0$ and $Fs_{90}Rh_{10}$ ($Fs_{95}Rh_5$ bulk composition). The abscissa shows moles Mn/2(Fe + Mn).

is independent of P and T for a disordered (model 1a) and completely ordered (model 1b) pyroxene and assumes further that fayalite-tephroite solid solutions are ideal ($\gamma^{oliv}_{Fe_2SiO_4} = 1$) for models 1a and 1b. These constant-K_D models require that either $\gamma^{opx}_{FeSiO_3}$ decreases with decreasing T or, in the event Fe-Mn olivine solutions are also somewhat non-ideal (1c), that $\gamma^{oliv}_{Fe_2SiO_4}$ increases *much* more rapidly than $\gamma^{opx}_{FeSiO_3}$ with decreasing T. Greater deviations from ideality might be predicted for Fe-Mn pyroxenes because of the substantial miscibility gap between $FeSiO_3$ and $MnSiO_3$, compared to Fe-Mn olivines for which there is complete solid solution between Fe_2SiO_4 and Mn_2SiO_4. However, that Fe-Mn pyroxenes should become more ideal at lower temperature or that the non-ideality of olivine increase more rapidly than orthopyroxene with decreasing temperature seem somewhat unlikely based on data of other silicate solutions. Models 2a and 2b show that if Fe-Mn solutions in orthopyroxene and olivine are ideal, or nearly so, a model with a temperature-dependent K_D might fit the data. Unfortunately the required K_D values are near the lower limit allowed by the data. At 900°C, the inferred models with K_D's of 1.18 (2a) and 1.15 (2b) are permitted by the data only if errors in the microprobe data are considered. The difference between K_D of 1.15 and 1.20 (the lower half-reversal of the K_D at 900°C) is equivalent to a difference of $X^{opx}_{Fe} = \pm 0.002$ for Fe + Mn = 2.0, which is beyond the accuracy and precision of the microprobe analyses used to infer the K_D. Nevertheless the K_D's required by models 2a and 2b are significantly below typical values (1.3–1.4) obtained from natural pairs [6–8] that appear to have equili-

TABLE 5

Iron site occupancies in Fe, Mn orthopyroxenes from Mössbauer spectra

Composition	Temperature (°C)	Fe^{2+} content		Random	Deviation from	
		M1	M2		Mn in M2	Mn in M1
$Fe_{1.00}$	900	0.99 (1)	1.01 (1)	1σ	–	–
$Fe_{0.95}Mn_{0.05}$	750	0.98 (1)	0.92 (1)	3σ	2σ	8σ
$Fe_{0.95}Mn_{0.05}$	900	0.98 (1)	0.92 (1)	3σ	2σ	8σ
$Fe_{0.90}Mn_{0.10}$	750	0.88 (2)	0.92 (2)	2σ	8σ	5σ
$Fe_{0.90}Mn_{0.10}$	900	0.92 (1)	0.88 (1)	2σ	6σ	9σ

TABLE 6

Activity models for Fe-Mn pyroxenes

Constant K_D models

Temperature (°C)	Model 1a		Model 1b		Model 1c	
	K_D = 1.2	K_D = 1.4	K_D = 1.2	K_D = 1.4	K_D = 1.4	
	Mn disordered in opx		Mn ordered in opx		Mn ordered in opx	
	$\gamma^{opx}_{FeSiO_3}$	$\gamma^{opx}_{FeSiO_3}$	$\gamma^{opx}_{FeSiO_3}$	$\gamma^{opx}_{FeSiO_3}$	$\gamma^{opx}_{FeSiO_3}$	$\gamma^{oliv}_{Fe_2SiO_4}$
700	0.998	1.005	0.999	1.014	1.026	1.006
800	1.000	1.007	1.002	1.017	1.025	1.004
900	1.001	1.008	1.005	1.020	1.024	1.002
1000	1.003	1.010	1.007	1.023	1.023	1.000

Variable K_D models assuming $\gamma^{opx}_{FeSiO_3} = \gamma^{oliv}_{Fe_2SiO_4} = 1$

Temperature (°C)	Model 2a Mn disordered in opx	Model 2b Mn ordered in opx
	K_D	K_D
700	1.26	1.21
800	1.21	1.18
900	1.18	1.15
1000	1.17	1.14

Variable K_D models assuming $\gamma^{opx}_{FeSiO_3} = 1.007\ \gamma^{oliv}_{Fe_2SiO_4} = 1$

Temperature (°C)	Model 3a Mn disordered in opx	Model 3b Mn ordered in opx
–	K_D	K_D
700	1.46	1.32
800	1.40	1.27
900	1.38	1.24
1000	1.35	1.21

brated between 750 and 850°C. It is possible that components outside the Fe_2SiO_4-Mn_2SiO_4-SiO_2 system are affecting the K_D of natural coexisting phases, causing them to appear slightly higher than the synthetic phases. If the equilibrium K_D is larger, perhaps 1.35 ± 0.05, then models 3a or 3b might fit the data. These models require that K_D increase with decreasing T and that Fe-Mn orthopyroxene be somewhat non-ideal. Similar but more complicated models wherein $\gamma^{opx}_{FeSiO_3}$ and $\gamma^{oliv}_{Fe_2SiO_4}$ vary with temperature and $\gamma^{opx}_{FeSiO_3} > \gamma^{oliv}_{Fe_2SiO_4}$ can be constructed. But any such model yet considered requires an increase in K_D with decreasing temperature. Our data allow changes in K_D with temperature but tighter reversals are necessary to confirm or deny them. Based on the present experimental data and data from natural minerals, it would appear that the mixing of 10 mole % $MnSiO_3$ in $FeSiO_3$ may be somewhat non-ideal. However, nothing definitive can be stated without tighter reversals of $K_D{}^{opx\text{-}oliv}_{Mn\text{-}Fe}$ and accurate activity data for fayalite-tephroite solid solutions.

4. Application in field areas

Manganese is not commonly the most significant impurity affecting the stability of Fe-rich ortho-

pyroxenes. Typical proportions of $MnSiO_3$ in ferrosilite-rich pyroxenes range between 1 and 4 mole % as a cursory look at analyses of pyroxenes from field areas such as the Adirondacks [1], Nain [6], Minnesota [7], and the Labrador Trough [9] will show. In these areas, pressures inferred from the orthopyroxene barometer can be revised downward to account for the effect of manganese, although the magnitude of the correction will be small. Unfortunately, pressures in some of these areas might still be somewhat uncertain because of the uncalibrated effect of other components such as Ca, Ti, Al, and Fe^{3+}. In the Adirondacks, there is typically less than 3 mole % rhodonite in orthopyroxene and tephroite in fayalitic olivine, requiring <0.35 kbar correction. However, there are a few field areas in which ferrosilite-rich pyroxenes and/or fayalitic olivine + quartz have significant amounts of Mn. Frisch and Bridgwater [8] describe orthopyroxene-olivine-quartz assemblages from South Greenland with up to 6 mole % $MnSiO_3$ in the orthopyroxene. Pressures of 3.9 to 5.4 kbar were estimated (for temperatures of 750–900°C), but the writers noted that the pressures might be in error because of the effects of components outside the Fe_2SiO_4-Mg_2SiO_4-SiO_2 system. The experimental work described here and in the preceding paper indicates that emplacement pressures for the intrusions described by Frisch and Bridgwater are 1–2 kbar lower than previously estimated.

In the Lofoten area of Norway, Krogh [4] and Ormaasen [10] report Fe-rich orthopyroxenes where Mn is the major diluent. In fact, a manganoan orthopyroxene that coexists with pyroxferroite reported by Krogh [4] is essentially $Fs_{75}Rh_{22}$, with all other components making up only 3 mole %. Extrapolation of our data for this pyroxene requires minimum pressures of approximately 9 kbar at 800°C or 10.5 kbar at 950°C. In similar rocks less than 70 km away from those reported by Krogh, Ormaasen reports orthopyroxenes ($Fe_{87-91}Rh_{5-8}En_{1-2}Wo_{1-2}$) coexisting with fayalitic olivine + quartz in textures which suggest that orthopyroxene is growing at the expense of olivine + quartz. Our data require pressures near 8 kbar at 700°C or 9 kbar at 800°C; these pressures are somewhat lower than those previously estimated. Other Fe-rich orthopyroxenes with significant rhodonite solid solution have been reported by Tsuru and Henry [11], Saxen [12], and Sundius [13], but they contain relatively large amounts of enstatite, wollastonite, and tschermak's component, which make pressure estimates uncertain. Experimental calibration of the effect of these other components would be useful.

Acknowledgements

The writers are grateful for and acknowledge the support of the Geochemistry Section of the National Science Foundation grants EAR76-22330 and EAR78-16413 to A.L.B., EAR75-22388 and EAR78-23568 to E.J.E., DES74-19918 to W.A.D., Geological Society of America grant No. 2168-77 to S.R.B. and the University of Michigan, Turner Funds grants to S.R.B. The writers wish to thank Dr. Jack C. Allen (Department of Geology and Geography, Bucknell University) and Mr. Robert Jones (Department of Earth and Space Sciences, UCLA) for their assistance in several aspects of this research. Mr. Derwin Bell drafted the line drawings.

References

1 S.R. Bohlen, E.J. Essene and A.L. Boettcher, Reinvestigation and application of olivine-quartz-orthopyroxene barometry, Earth Planet. Sci. Lett. 47 (1980) 1.
2 D. Smith, Stability of iron-rich orthopyroxene, Carnegie Inst. Washington Yearb. 68 (1969) 229.
3 D. Smith, Stability of the assemblage iron-rich orthopyroxene-olivine-quartz, Am. J. Sci. 271 (1971) 370.
4 E.J. Krogh, Origin and metamorphism of iron formations and associated rocks, Lofoten-Vesterålen, N. Norway, I. The Vestpolltind Fe-Mn deposit, Lithos 10 (1977) 243.
5 L.H. Cohen and W. Klement, Jr., High-low quartz inversion: determination to 35 kilobars, J. Geophys. Res. 72 (1967) 4245.
6 J.H. Berg, Regional geobarometry in the contact aureoles of the anorthositic Nain Complex, Labrador, J. Petrol. 18 (1977) 399.
7 B. Bonnichsen, Metamorphic pyroxenes and amphibolites in the Biwabik Iron Formation, Dunka River Area, Minnesota, Mineral. Soc. Am. Spec. Paper 2 (1969) 217.
8 T. Frisch and D. Bridgwater, Iron- and manganese-rich minor intrusions emplaced under late-orogenic conditions in the Proterozoic of South Greenland, Contrib. Mineral. Petrol. 57 (1976) 25.
9 C. Klein, Regional metamorphism of Proterozoic iron formation, Labrador Trough, Canada, Am. Mineral. 63 (1978) 898.

10 D.E. Ormaasen, Petrology of the Hopen mangerite-charnockite intrusion, Lofoten, North Norway, Lithos 10 (1978) 291.
11 K. Tsuru and N. Henry, An iron rich optically positive hypersthene from Manchuria, Mineral. Mag. 24 (1937) 527.
12 M. Saxen, Om manganiarnmalmfyndighetene i Vittinki, Fennia 45 (1925) 18.
13 N. Sundius, Uber den sogenannten Eisenathophyllit der Eulysite, Arb. Sver. Geol. Unders. 26 (1932) 2.
14 G.M. Bancroft, Mössbauer Spectroscopy (McGraw-Hill, London, 1973) 165–177; 212–221.
15 S. Ruby, Mössbauer Effect Methodology, Vol. 8, I.J. Gruverman, ed. (Plenum Press, New York, N.Y.) 263–276.